Molecular Crystals and Liquid Crystals

ISSN: 1542-1406 (Print) 1563-5287 (Online) Journal homepage: http://www.tandfonline.com/loi/gmcl20

Dielectric and Electro-Optical Properties of Polymer-Stabilized-Blue-Phase Cells

Hsuan-Tsung Hsu, Po-Chang Wu & Wei Lee

To cite this article: Hsuan-Tsung Hsu, Po-Chang Wu & Wei Lee (2015) Dielectric and Electro-Optical Properties of Polymer-Stabilized-Blue-Phase Cells, Molecular Crystals and Liquid Crystals, 617:1, 92-99, DOI: 10.1080/15421406.2015.1076331

To link to this article: http://dx.doi.org/10.1080/15421406.2015.1076331

Published online: 07 Oct 2015.

Mol. Cryst. Liq. Cryst., Vol. 617: pp. 92–99, 2015

ISSN: 1542-1406 print/1563-5287 online
DOI: 10.1080/15421406.2015.1076331

Dielectric and Electro-Optical Properties of Polymer-Stabilized-Blue-Phase Cells

HSUAN-TSUNG HSU, PO-CHANG WU, AND WEI LEE*

College of Photonics, National Chiao Tung University, Tainan, Taiwan

This study focuses on the dielectric and phase behaviors of monomer/blue-phase-liquid-crystal (BPLC) composites before and after photopolymerization. At a fixed frequency of 1 kHz, where the dielectric behavior is dominated by the orientation of LC molecules, our experimental results indicate that the phase transition temperatures and, in turn, the temperature ranges of blue phases in BPLC cells can be distinguished by using the second-order derivative of dielectric permittivity with respect to the temperature. In considering the typical driving methods for display applications, the electro-optical performance of polymer-stabilized BPLC cells driven by in-plane and vertical-field switching is investigated and briefly compared.

Keywords Blue-phase liquid crystals; dielectric spectroscopy; phase transition temperatures

Introduction

Blue-phase (BP) liquid crystals (LCs) reveal alluring features of optical isotropy in the voltage-off state and submillisecond response time, allowing the realization of next-generation display technologies such as alignment-layer-free and polarizer-free fabrication processes and the wide-viewing-angle, field-sequential color display. Moreover, BPLCs are potential for applications in photonic devices due to their three-dimensional (3-D) helical structure with periodicity of the order of visible wavelengths. Unfortunately, BPLCs are known to have some intrinsic problems, including low transmittance, large hysteresis, high operating voltage, residual birefringence, and narrow BP temperature range, that hinder their practical uses [1, 2]. Among developed BPLC technologies, polymer stabilization has been a well-known approach for widening the temperature range of a BP. In general, BPs are formed by adding chiral molecules to impose on the host nematic molecules a regular array of double twist cylinders separated through a network of disclination lines. Forming polymers in polymer-stabilized (PS)-BPLCs plays an important role in stabilizing the line defects in which rotational symmetry is violated [3–5]. It has been demonstrated that the PS-BPLC allows the BP temperature range to extend to more than 60 K, including room temperature [4]. As a result, PS-BPLCs have attracted considerable attention from the point

*Address correspondence to Wei Lee, Institute of Imaging and Biomedical Photonics, College of Photonics, National Chiao Tung University, 301 Gaofa 3rd Rd., Guiren Dist., Tainan 71150, Taiwan. E-mail: wlee@nctu.edu.tw

Color versions of one or more of the figures in the article can be found online at www.tandfonline.com/gmcl.

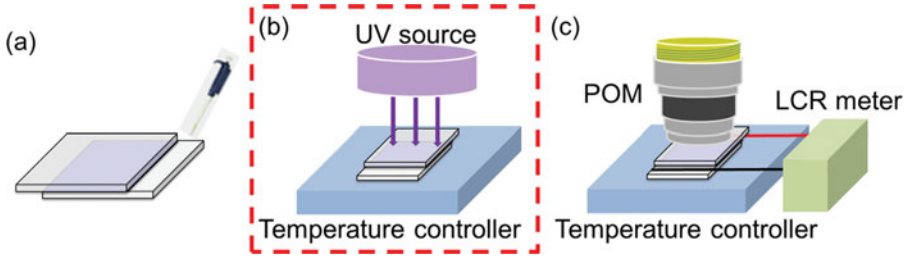

Figure 1. Schematic of sample fabrication and measurement. (a) Injection of the mixture into a glass cell. (b) Cooling to the BP-I phase and photopolymerization of the sample with UV light. (c) Observing the cell before and after polymerization.

of view of potential applications in phase modulator devices [6, 7], field-sequential displays [8, 9], and 3-D tunable photonic crystals [10, 11].

In view of fabrication steps of conventional PS-BPLCs, the photopolymerization process is accomplished at a critical temperature where the LC cell reveals BPs. As such, specifications including precise phase transition temperatures and temperature ranges of BPs are essential for practical PS-BPLCs. Thus far, a number of methods for the determination of phase sequences of BPLCs have been proposed, including the Kössel diagram [12], selective-reflection measurement [13], and differential scanning calorimetry [14]. In our previous study, dielectric spectroscopy has been used to explore the polarization and relaxation behaviors of LC molecules [15, 16]. Since the dielectric properties of LCs are dependent of the surrounding temperature, the transition temperature between two neighboring phases can be obtained by observing the variation of the real-part dielectric constant ε'' in the temperature-dependent dielectric plot of a LC. Along this line, the present work presents a feasible and reliable method for identification of the phase transition temperatures of a BPLC dispersed with a monomer, before and after photopolymerization, by means of temperature-dependent dielectric spectroscopy. In addition, the phase transitions are monitored with simultaneous observations of their optical textures using a polarizing optical microscope (POM). Finally, electro-optical properties manifested by the voltage–transmittance curves of several PS-BPLC cells driven by the in-plane switching (IPS) and the vertical-field switching (VFS) are compared and discussed.

Experimental

Fabrication Process of Monomer/BPLC and PS-BPLC Samples

The monomer/BPLC mixture was made of a BPLC material doped with two kinds of ultraviolet (UV)-curable monomers (1741 and BJ0050) and a photoinitiator (BJ0048). The weight ratios of 1741, BJ0050 and BJ0048 to the BPLC are 4.5, 2.9 and 0.3 wt%, respectively. Note that the BPLC was concocted by incorporating a chiral agent (0933) at 3.6 wt% into a nematic LC (P70-003) host. The birefringence Δn and dielectric anisotropy $\Delta\varepsilon$ of the nematic host are $\Delta n = 0.156$ at the wavelength of 589 nm and temperature of 20°C and $\Delta\varepsilon = 33.6$ at the frequency of 1 kHz and temperature of 25°C. All of the above-mentioned materials were provided by Shijiazhuang Slichem Liquid Crystal Materials Co., Ltd. (SLICHEM), a main LC material supplier located in China. Figure 1 shows the fabrication process of the PS-BPLCs.

Table 1. Cell parameters of various BPLC samples

Sample	Cell gap (μm)	Electrode type	Inter-digital electrode spacing (μm)
A	4.5	ITO	
B	5.5	ITO	
C	8.0	ITO	
D	5.5	Inter-digital	6
E	5.5	Inter-digital	10
F	8.0	Inter-digital	6
G	8.0	Inter-digital	10

ITO: The meaning of ITO here represents the substrate with ITO electrode material covering the whole area.

In this study, seven samples, designated samples A to G, with distinct cell parameters were fabricated as listed in Table 1. Here, indium–tin-oxide (ITO)-coated substrates were used in samples A to C while samples D to G have inter-digital electrodes deposited on one of the two assembled substrates. It is worth mentioning that all samples were fabricated without coating any alignment film on the substrate. Except for sample A specifically made for dielectric studies, the remaining samples with polymer stabilization (B through G) were used for the investigation of electro-optical properties of PS-BPLCs. The resulting monomer/BPLC mixture was injected into empty cells by capillary action in its isotropic phase (Fig. 1(a)). To carry out the photopolymerization process for forming a PS-BPLC, a monomer/BPLC sample was cooled from the isotropic phase with a rate of 0.1°C/min using a temperature controller (Linkam T95-PE) and then fixed at the temperature where the sample exhibits the BP-I phase. Later, the sample in BP-I was irradiated with UV light at the wavelength of 365 nm and the intensity of 4 mW/cm^2, for 8 minutes, as shown in Fig. 1(b). The phase transition temperature of two adjacent mesophases in each cell was determined according to the temperature-dependent dielectric data and optical texture change, monitored with an LCR meter and a POM, respectively. The setup

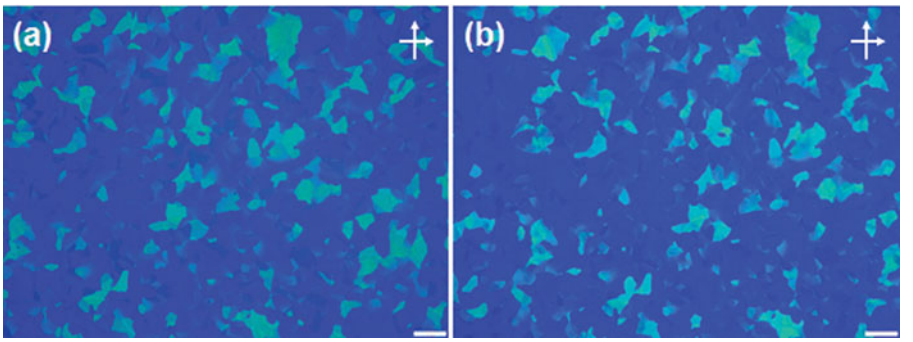

Figure 2. POM images of sample A in BP-I at 65°C (a) before and (b) after photopolymerization.

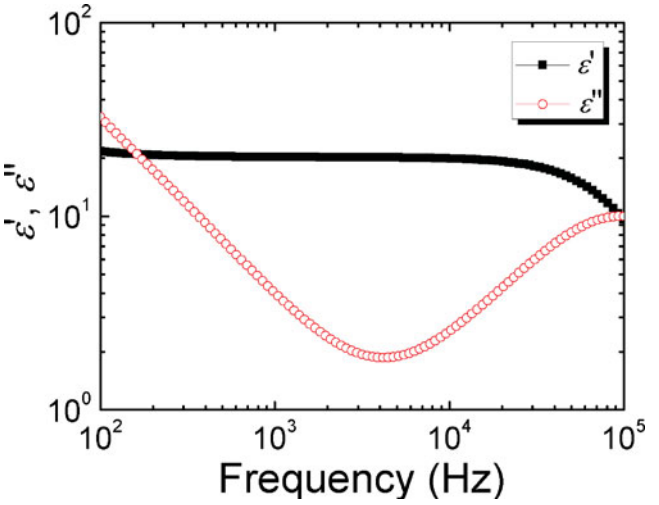

Figure 3. Dielectric constants of a BPLC (sample A) in BP-1 at 65°C before UV curing.

for dielectric measurement and the simultaneous observation of optical textures is illustrated in Fig. 1(c). Figure 2 exemplarily shows some POM images of sample A at a fixed temperature in BP-1 prior to and after polymerization. The resulting platelet textures preliminarily indicate the stabilization of BP-I in the sample through the photopolymerization process.

Measurements

The temperature-dependent dielectric data measured for studying phase behaviors of a monomer/BPLC cell before and after UV exposure were acquired with a precision LCR meter (Agilent E4980A), in the frequency range of 10^2–10^5 Hz, as well as the temperature controller mentioned above. It should be noted that only sample A was used in this dielectric measurement. The probe voltage used was 0.1 V_{rms} in the sinusoidal waveform, which was smaller than the Fréedericksz-transition voltage of the BPLC. The temperature range for dielectric measurement was set between 40 and 100°C with an accuracy of ±0.01°C. Furthermore, the POM observation was also made to determine the transition temperature between two adjacent phases of sample A. The optical textures at decreasing temperatures of sample A before and after photopolymerization were obtained with an Olympus BX51TRF microscope.

The voltage-dependent transmission (V–T) curves of the PS-BPLC samples (B through G) were measured at room temperature using a He–Ne laser operating at the wavelength of 632.8 nm, an arbitrary function generator (Tektronix AFG-3022B), and an amplifier (TREK Model 603). The voltage pulses were supplied in square waveform at frequency of 1 kHz. For the IPS mode, samples with inter-digital electrodes (i.e., samples D to G) were situated between crossed polarizers and the direction of electrodes was oriented at 45° with respect to the transmission axis of either polarizer. In this case the probe laser beam was normally incident onto a sample whereas the laser light was incident to a VFS-mode cell at an oblique angle of 45° as used for samples B and C.

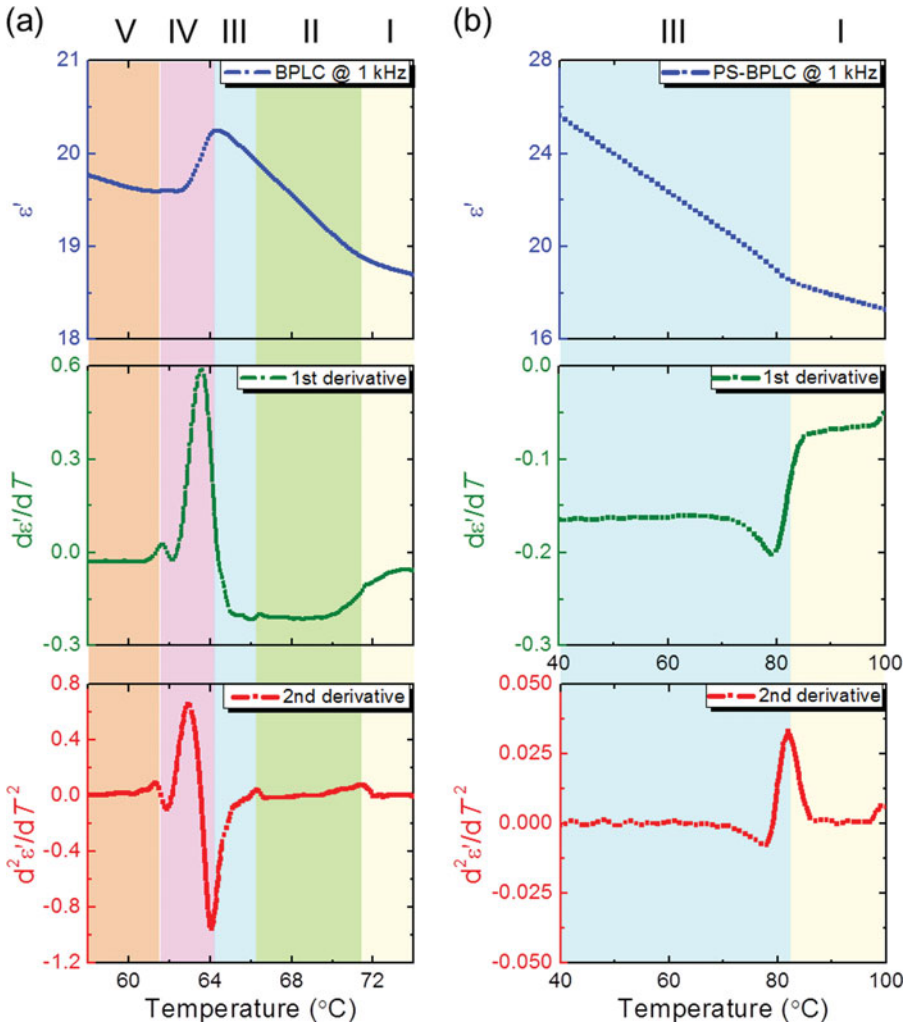

Figure 4. Temperature dependence of dielectric permittivity $\varepsilon'(T)$ and the first and second derivatives of sample A at 1 kHz (a) before and (b) after photopolymerization.

Results and Discussion

Temperature-Dependent Dielectric Functions

Figure 3 reveals an example of the complex dielectric spectrum of the monomer/BPLC cell (sample A) at a specific temperature T. The complex dielectric function is represented by $\varepsilon^* = \varepsilon' - i\varepsilon''$, where ε' is the real part and ε'' is the imaginary part. In the low-frequency (f) regime (100–500 Hz), the complex dielectric function is dominated mainly by the ionic effect in which the ε' and ε'' functions behave as $f^{-3/2}$ and f^{-1}, respectively. In the frequency range between 500 Hz and 10 kHz, the value of ε' is attributable to the orientation of LC molecules, which is independent of f. According to the T dependence of the molecular ordering, the phase transition can be identified by means of the variation of ε' with T in this frequency range (500 Hz and 5 kHz). Accordingly, the T-dependent dielectric permittivity at

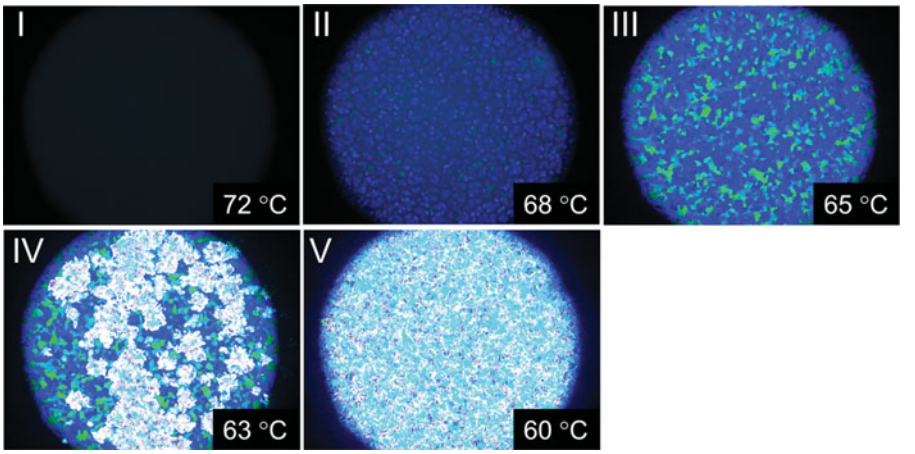

Figure 5. Optical textures of sample A at five temperatures (based on Fig. 4) before UV exposure.

$f = 1$ kHz can be established to study phase behaviors of BPLCs. Noticeably, the dielectric data beyond 5 kHz as shown in Fig. 3 should not be considered for analysis owing to the pseudo-relaxation fundamentally caused by the cell geometry.

Figure 4 shows the T-dependent dielectric constants $\varepsilon'(T)$, the first- and second-order derivatives of ε' with respect to T of sample A before and after UV exposure. In the case of sample A before UV exposure (i.e., the monomer/BPLC mixture), as shown in Fig. 4(a), the transformation between adjacent phases leads to the generation of a local extremum in the first- and second-order derivatives of T-dependent dielectric data and, thus, simply sheds light on the phase transition temperature. The approach based on the data of $\varepsilon'(T)$ to determine the phase transition temperature has previously been proposed for LCs via the first derivative ($d\varepsilon'/dT$) [15]. However, it is difficult here to distinguish the phase change from the isotropic phase to BP-II and from BP-II to BP-I using the $d\varepsilon'/dT$ data (Fig. 4(a)). This is presumably due to the similar double-twist configurations in BPs to the isotropic structure in the liquid phase. With further performing the second derivative

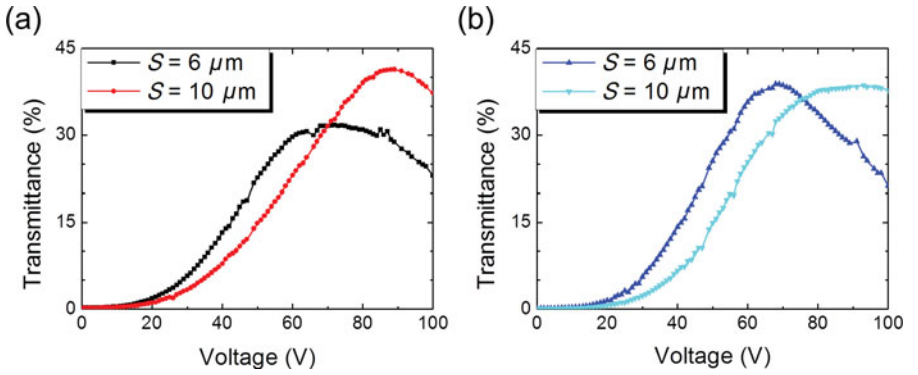

Figure 6. V–T curves of (a) samples D ($S = 6$ μm) and E ($S = 10$ μm) with $d = 5.5$ μm and (b) samples F ($S = 6$ μm) and G ($S = 10$ μm) with $d = 8.0$ μm. Here, S and d represent the separation distance between two adjacent electrodes and the cell gap of samples, respectively.

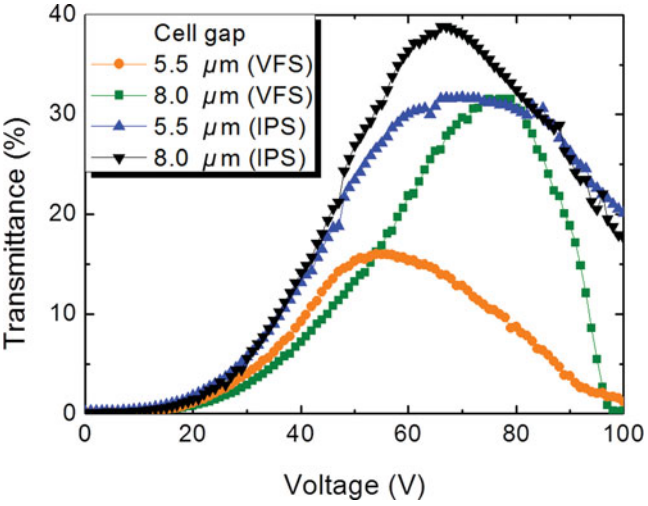

Figure 7. *V–T* curves of two VFS-mode cells—sample B ($d = 5.5$ μm) and sample C ($d = 8.0$ μm)—and two IPS-mode cells—sample D ($d = 5.5$ μm) and sample F ($d = 8.0$ μm) with $S = 6.0$ μm. All of the four are PS-BPLC samples.

of ε' with respect to T ($d^2\varepsilon'/dT^2$), one can see four features located at 71.4, 66.3, 64.1 and 61.7°C in the temperature regime between 55 and 75°C. Compared with the results of POM observations at given temperatures (Fig. 5) it is obvious that these features correspond to the phase transition temperatures of the mesogenic material. Consequently, the phase sequence of sample A before UV exposure can be divided into five regions. These regions on the cooling process are (I) Isotropic, (II) BP-II, (III) BP-I, (IV) BP-I + CLC, and (V) CLC, where CLC stands for the cholesteric phase. The deduced BP temperature range covering both BP-II and BP-I is 7.3°C for sample A before UV exposure. After polymerization, only one peak at 82°C is exhibited in the curve of $d^2\varepsilon'/dT^2$ for sample A (Fig. 4(b)). The two regions divided by the peak are the isotropic phase and BP-I. Note that the temperature range of BP-I in polymer-stabilized sample A can be extended from 82°C down to at least –40°C, indicating that polymer stabilization indeed helps broaden the BP range [4]. Here as a reminder, all of the characteristic temperatures mentioned above are extremely close to the results obtained from optical texture observations.

Voltage-Dependent Transmittance (V–T) Curves

With regard to the IPS-mode PS-BPLCs, Fig. 6 illustrates the *V–T* curves of samples D to G having identical electrode width of $W = 10$ μm. Consider samples D and E with the same cell gap of $d = 5.5$ μm first. The experimental data disclose that the on-state voltage V_{on}, corresponding to the highest transmittance in the *V–T* curve, for sample D with electrode-separation distance of $S = 6$ μm is 59.5 V, which is substantially lower than that of sample E with $S = 10$ μm ($V_{on} = 78.5$ V) as shown in Fig. 6(a). This phenomenon stems from the bending of electric field in the area far from the electrodes as S increases. The same dependence of the on-state voltage on the electrode spacing can also be found for samples F and G with a larger cell gap ($d = 8.0$ μm) as depicted in Fig. 6(b). The experimental results show that the operation voltage of IPS-mode PS-BPLC is insensitive to the cell gap.

To examine the electro-optical properties of PS-BPLCs under a uniform electrical field and compare them with those samples driven by an in-plane field, Fig. 7 shows the measured *V–T* curves of VFS-mode PS-BP samples (samples B and C) as well as IPS-mode PS-BPLC samples (samples D and F). For VFS-mode PS-BPLC samples, V_{on} increases with increasing cell gap, which is in agreement with the understanding for conventional LC displays driven by vertical fields. In comparison with the IPS-mode PS-BPLC sample with $d = 5.5$ μm and $S = 6$ μm (i.e., sample D), V_{on} of the VFS-mode cell with the same cell gap (sample B) is lower. The result turns opposite for the cells with $d = 8.0$ μm as shown in Fig. 7. The transmittance of the PS-BPLC samples with IPS electrodes is higher in general than that with conventional electrodes for VFS under the experimental conditions for this study.

Conclusions

While all of the attractive research surrounds the BPLC in the field of LC, this paper puts forward a preliminary study to determine the phase transition temperatures of BPLCs by employing dielectric spectroscopy. We demonstrated that the second-order derivative of real-part dielectric permittivity at 1 kHz enables determination of the temperature range of BPs with high precision. In addition, the phase sequence of a BPLC can clearly be defined through the temperature-dependent dielectric measurement together with the observation using a POM on the cooling process. It was found from the electro-optical properties of PS-BPLC cells that the transmittance of the PS-BPLC samples with IPS electrodes is significantly higher than that with VFS operation under the experimental conditions in this study.

Funding

This work was financially supported by the Southern Taiwan Science Park Bureau, Ministry of Science and Technology, Taiwan, through Grant No. 102GE02.

References

[1] Haseba Y., & Kikuchi H. (2007). *Mol. Cryst. Liq. Cryst.*, *470*, 1.
[2] Meiboom S., Sethna J.-P., Anderson P.-W., & Brinkman W.-F. (1981). *Phys. Rev. Lett.*, *46*, 1216.
[3] Coles, H.-J., & Pivnenko, M.-N. (2005). *Nature*, *436*, 997.
[4] Kikuchi, H., Yokota, M., Hisakado, Y., & Kajiyama, T. (2002). *Nature Mater.*,*1*, 64.
[5] Voloschenko, D., Pishnyak, O.-P., Shiyanovskii, S.-V., & Lavrentovich, O.-D. (2002). *Phys. Rev. E*, *65*, 060701.
[6] Lu, S.-Y., & Chien, L.-C. (2010). *Opt. Lett.*, *35*, 562.
[7] Yan, J., Li, Y., & Wu, S.-T. (2011). *Opt. Lett.*, *36*, 1404.
[8] Chen, K.-M., Gauza, S., Xianyu, H.-Q., & Wu, S.-T. (2010). *J. Disp. Technol.*, *6*, 318.
[9] Kim, M., Kang, B.-G., Kim, M.-S., Kim, M.-K., Kumar, P., Lee, M.-H., Kang, S.-W., & Lee, S.-H. (2010). *Curr. Appl. Phys.*, *10*, e118.
[10] Coles, H., & Morris, S. (2010). *Nature Photonics*, *4*, 676.
[11] Yokoyam, S., Mashiko, S., Kikuchi, H., Uchida, K., & Nagamura, T. (2006). *Adv. Mater.*, *18*, 48.
[12] Crooker, P.-P. (2001). *Chirality in Liquid Crystals*, Springer: New York.
[13] Bergmann, K., Pollman, P., Scherer, G., & Stegemeyer, H. (1979). *Z. Natugorsch.*, *34A*, 253.
[14] Armitage, D., & Price, F.-P. (1975). *J. Phys.*, *36*, C1–133
[15] Wu, P.-C., & Lee, W. (2013). *Appl. Phys. Lett.*, *102*, 162904.
[16] Lin, F.-C., Wu, P.-C., Jian, B.-R., & Lee, W. (2013). *Adv. Cond. Mat. Phys.*, *2013*, 271574.